Anal. Bioanal. Electrochem., Vol. 11, No. 7, 2019, 930-942

Analytical & Bioanalytical Electrochemistry

2019 by CEE
www.abechem.com

Full Paper

X-Fe_2O_4-Buckypaper-Chitosan Nanocomposites for Nonenzymatic Electrochemical Glucose Biosensing

Nadia Farsaei Vahid,[1] Mohammad Reza Marvi,[1] Mohammad Reza Naimi-Jamal,[1] Seyed Morteza Naghib[2,*] and Ali Ghaffarinejad[3]

[1]Research Laboratory of Green Organic Synthesis & Polymers, Department of Chemistry, Iran University of Science and Technology (IUST), P.O. Box 16846-13114 Tehran, I. R. Iran
[2]Nanotechnology Department, School of Advanced Technologies, Iran University of Science and Technology (IUST), Tehran, Iran
[3]Research Laboratory of Real Samples Analysis, Department of Chemistry, Iran University of Science and Technology (IUST), Iran

*Corresponding Author, Tel.: +982173225830; Fax: +982177240380
E-Mail: naghib@iust.ac.ir

Received: 13 January 2019 / Received in revised form: 3 July 2019 / Accepted: 13 July 2019 / Published online: 31 July 2019

Abstract- The exploitation of undemanding modifications needed for rising the sensitivity and functionality of nanobiosensors is still remaining a challenge. Conventional enzyme-based sensors propose favorably selective and sensitive determination of glucose at the outlay of low stability. Thus, promoting the comfortable, sensitive, rapid and consistent strategies play an impressive role for determining the human glucose level. Here, a new nanocomposite, X-Fe_2O_4-Buckypaper-Chitosan (X=Fe_3O_4, $ZnFe_2O_4$ and $CuFe_2O_4$), was scrutinized to find an appropriate substrate for nonenzymatic biosensing. The nanocomposites were characterized by Fourier transform infrared spectroscopy (FTIR), X-ray diffraction (XRD) and Field emission scanning electron microscopy (FESEM). The average particle size of all nanoparticles was lower than 100 nm. The Cu-Fe_2O_4-buckypaper-chitosan composite has shown a significant electrochemical behavior compared with the other composites. The biosensor was applied to detect glucose with a linear range of 0.25×10^{-3}–17×10^{-3} M and detection limit is 0.025 μM. The biosensor presented reasonable results for glucose at applied potential of 0.575 V with a fast response time (<4 s). This is the first research on the X-Fe_2O_4-Buckypaper-Chitosan biosensing application and its abovementioned sensing characteristics are comparable with those heretofore reported developments.

Keywords– Buckypaper, Magnetic nanoparticles, Chitosan nanocomposite, Electrochemical behavior; Glucose biosensor

1. INTRODUCTION

Carbon-based nanostructures have attracted much attention due to their excellent features such as mechanical [1-3] and electrical [4,5] properties. Composite nanomaterials have shown unique characteristics [6,7] over many applications such as biosensors [8,9] and biodections of biomarkers [10,11]. Electroanalytical methods have been applied for synthesis an electrochemical sensor and biosensor for measuring and quantification of enormous biomarker species [12-15]. Having a high quality response to the electrochemical measurement has an impressive role in fabrication of efficacious, reliable, and perpetual devices that caused many protocols were developed to address several challenges [16-19]. Synthesis and fabrication of a tunable nanocomposite with suitable properties for biomedical analysis and biosenbsors is a big challenge [20,21]. BP is a thin film (5–25 μm) comprised of arranged ropes of nanotubes. Recently, BPs gain much attention among the other shape of carbon nanotubes because of its useful ability [22].

Chitosan is a plentiful natural biopolymer with significant features such as, biocompatibility, and non-toxic [23]. This organic material can be utilized to immobilize metal ions [24]. In this context, the combination of nanoparticle with chitosan has provided a chance to investigate the electrochemical behavior of sensor [19].

Glucose is an essential metabolite for living, especially in diabetic patients [25]. The novel nanocomposites provide new chances for studies of biosensors. Magnetic nanoparticle, such as Fe_3O_4, $CuFe_2O_4$ and $ZnFe_2O_4$ are the most versatile of the ferrites. Due to their high surface-to-volume ratios, they are very common material to increase electrochemical activities [26,27]. Electrodes amended with metallic nanoparticle show good performances in biosensing application [28].

Although enzyme-based biosensors propose sensitive and selective determination of glucose, the biosensors stability is extremely low [27]. Then, fabricating a steady, stable, sensitive, fast and reliable biosensor has a key role, yet to be challenged. In this paper, we synthesized BP with Tween 20 surfactant which showed more reasonable electrochemical performance than the other surfactant[29] and also composites of BP were synthesized with three different kinds of ferrites to investigate the electrochemical response. Due to most application of phases (Fe_3O_4, $CuFe_2O_4$ and $ZnFe_2O_4$) in biomedicine and immunology [30-32] we have worked on nanocomposite consist of these ferrites. Copper ferrite ($CuFe_2O_4$) contains ferromagnetic that can lead to have high electrochemical stability and being plentiful in nature [33] .

The electrochemical property of the electrode X-Fe_2O_4-buckypaper-chitosan (X-Fe_2O_4-BP-CH)/FTO film was studied in detail. The composite of $CuFe_2O_4$-BP-CH exhibited excellent electrochemical performance in measurement among the other ferrite. It appears that the presence of $CuFe_2O_4$-BP-CH may promote the features of the nanocomposite in current transfer as a biosensor. In following paragraphs, we report the results of X-Fe_2O_4-BP-CH

deposited onto FTO for electrochemical behavior investigation. The best nanocomposite, $CuFe_2O_4$-BP-CH, was used as a nonenzymatic sensor for detection glucose. The nanocomposite provided an outstanding capacity for designing a biosensor with remarkable performance via advanced glucose sensitivity for determining analyte and great selectivity among interfering species in real serum samples.

2. MATERIALS AND METHODS

2.1. Reagents and Apparatus

Potassium hexacyanoferrate, ethylene glycol, iron(ш) chloride, iron(п) chloride, zinc chloride, NH_4AC, acetic acid, CH and Tween 20 were provided from Sigma- Aldrich. electrochemical. Electrochemical measurements were executed in a 1 mM $K_3[Fe(CN)_6]$ and 0.05 M PBS solution by cyclic voltammetry (CV) at 100 mVs^{-1} and electrochemical impedance spectroscopy (EIS) at 0.23 V in electrochemical cell.

2.2. Preparation of X-Fe_2O_4 NPs

70 mL ethylene glycol with iron (ш) chloride and iron (п) chloride for X=Fe [34], copper (п) chloride for X=Cu [35], zinc chloride for X=Zn [36] was mixed in a mechanic stirrer to obtain a clean solution. Then, 2.312 g NH_4AC was added to the solution and sonicated for 40 min. The solution was put in an oven at 215 ˚C for 4h to get a black precipitate.

2.3. Preparation of BP

At first 10 mg SWCNT and using Tween 20 as a nonionic surfactant was added to 50 mL water. Resulting mixtures were ultrasoniced for 30 min then were stirred for 24 h. the final suspensions were filtered through a polytetrafluoroethylene (PTFE) membrane filter (0.45 μm pore size) and left to dry in room temperature [37].

2.4. Preparation of X-Fe_2O_4-BP-CH nanocomposite

1 g chitosan (CH) powder was mixed with 100 mL of 0.1 M acetic acid and stirred to get 1% clear solution of CH. Magnetic X-Fe_2O_4 and BP was ultra-sonicated at room temperature in the CH solution. Fig. 1 exhibits a schematic representation of the X-Fe_2O_4-BP-CH nanocomposite synthesis.

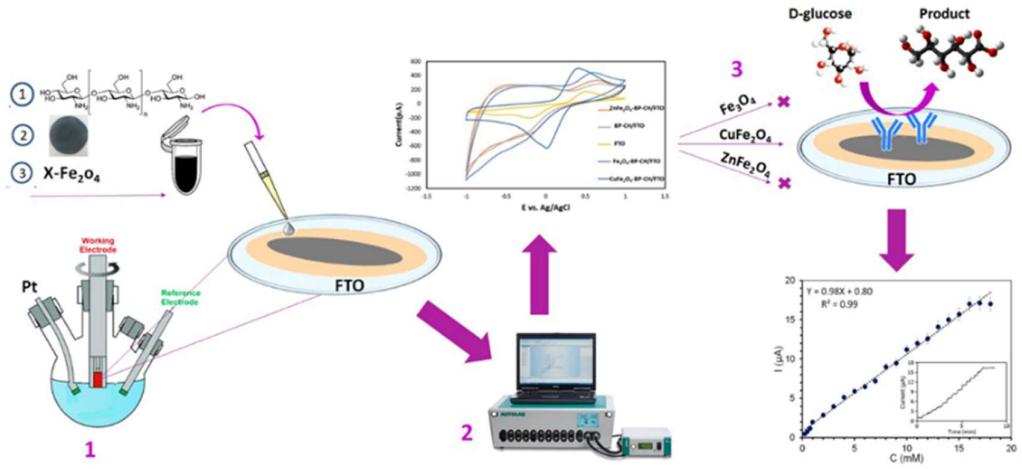

Fig. 1. Schematic representation of the synthesis of the composites and its electrochemical biosensing

3. RESULT AND DISCUSSION

3.1. Characterization of X-Fe_2O_4/BP nanocomposites

Fourier transform infrared (FTIR) was applied to analyze X-Fe_2O_4–BP-CH nanocomposite. Fig. 2a shows FTIR of BP without any sharp and distinctive peaks. In Fig. 2b, the broad bands in the range of 3600-3300 cm^{-1}, around 2920 cm^{-1}, around 1593 cm^{-1} , and at 1064 cm^{-1} indicate the presence of OH groups, N-H and C-O-C bonds in chitosan, respectively.

Compared with curves a and b, the peaks of hydroxyl, N-H, C-O-C groups and Fe–O bond (608.7 cm^{-1}) were all represented in curve c and another band in curve d and e at 490 cm^{-1} is related to octahedral group complex Zn^{2+}-O^{2-} and Cu^{2+}-O^{2-}.

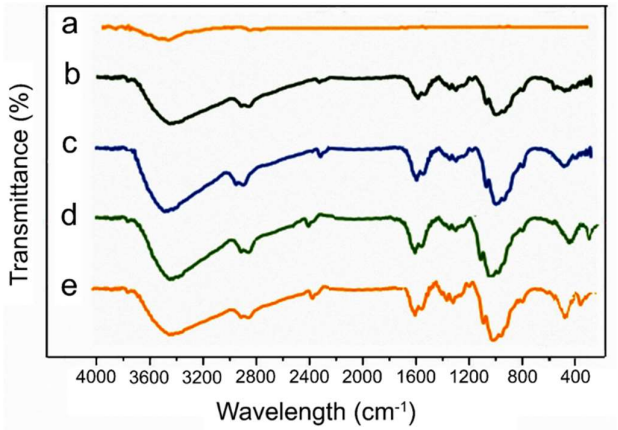

Fig. 2. FTIR of the (a) BP, (b) CH, (c) Fe_3O_4-BP-CH, (d) $ZnFe_2O_4$-BP-CH, (e) $CuFe_2O_4$-BP-CH

Surface morphological studies of X-Fe_2O_4-BP-CH/FTO electrode have been investigated using scanning electron microscopy. Fig. 3A shows the nanocomposite of $CuFe_2O_4$-BP-CH/FTO from different distance with homogeneous, smooth and crack-free surface which nanoparticle embedded in the BP nanotubes network uniformly with minimum aggregation. Figs. 3B depicts the Fe_3O_4-BP-CH/FTO nanocomposite surface features that during the formation of nanocomposite, the Fe_3O_4 nanoparticle were trapped in CNTs bundles with minimum agglomeration. Fig. 3C illustrates the uniform surface of $ZnFe_2O_4$/BP composite which is based on the homogeneous dispersion of $ZnFe_2O_4$ nanoparticles in the BP film. It appears that some of nanoparticles may be agglomerated. As a result, copper ferrites nanoparticles exhibit better surface for electron transfer with good distribution in particle and least agglomeration compared with cubic Zn and Fe ferrites nanoparticles.

We determined the size of the 50, 90 and 50 nanoparticles randomly. The particle size of most of the $CuFe_2O_4$, Fe_3O_4 and $ZnFe_2O_4$ particles were about 50-60, nm, 20-30 nm and 70-80 respectively. (Fig. 3A and B). In addition, the average size of the $CuFe_2O_4$, Fe_3O_4 and $ZnFe_2O_4$ nanoparticles was about 54.2, 28.31 and 78.21 nm.

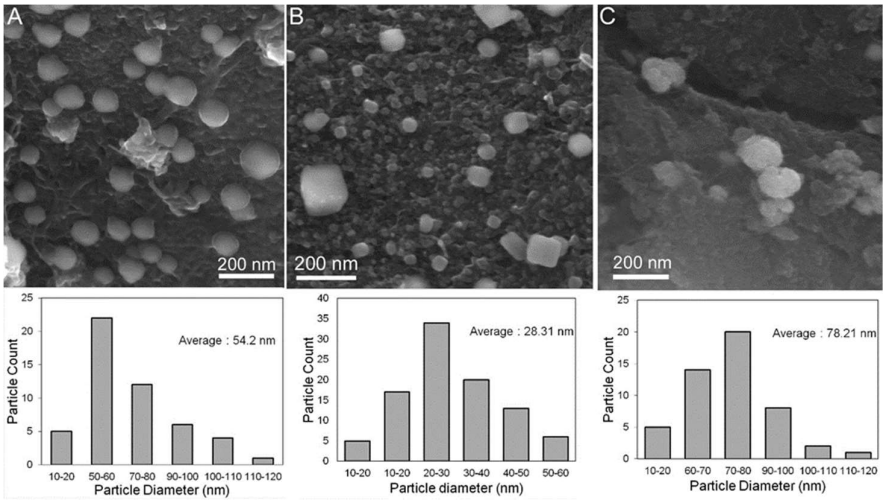

Fig. 3. FESEM image of the $CuFe_2O_4$-BP-CH composite from 200 nm and the nanoparticle size distribution of $CuFe_2O_4$ (A); FESEM image of the composite Fe_3O_4-BP-CH from 200 nm and the nanoparticle size distribution of Fe_3O_4 (B); FESEM images of the composite $ZnFe_2O_4$-BP-CH from 200 nm and the nanoparticle size distribution of $ZnFe_2O_4$ (C)

The XRD patterns of the nanoparticles are shown in Fig. 4. XRD confirms the formation of X-Fe_2O_4 nanoparticle. Strong Brag diffraction peaks are indicated in Fig. 5 that are alignment with the standard XRD pattern for $CuFe_2O_4$ (JPCDS No. 01-077-010) $ZnFe_2O_4$ (JPCDS No. 22-1012) and Fe_3O_4 (JPCDS No.65-3107), respectively. Fig. 5 exhibits VSM of

$ZnFe_2O_4$, Fe_3O_4 and $CuFe_2O_4$ nanoparticles. The VSM of $ZnFe_2O_4$ shows large saturation magnetization than others.

Electrochemical characterizations of bare FTO, BP-CH/FTO and X-Fe_2O_4-BP-CH/FTO nanocomposite electrodes as shown in Fig. 6. CVs were performed in 1 mM $K_3[Fe(CN)_6]$ and PBS 0.05 M (pH 7.4) at 100 mVs^{-1}.

$K_3[Fe(CN)_6]$ shows weak electrochemical behavior on the unmodified FTO with a high (ΔE=690 mV). The response of $K_3[Fe(CN)_6]$ at FTO increased to 232.4 μA at+0.49 V and -293.0 μA at -0.18 V because of the good conductivity of BP and also the cationic characteristics of CH, which accelerate the electrons transfer.

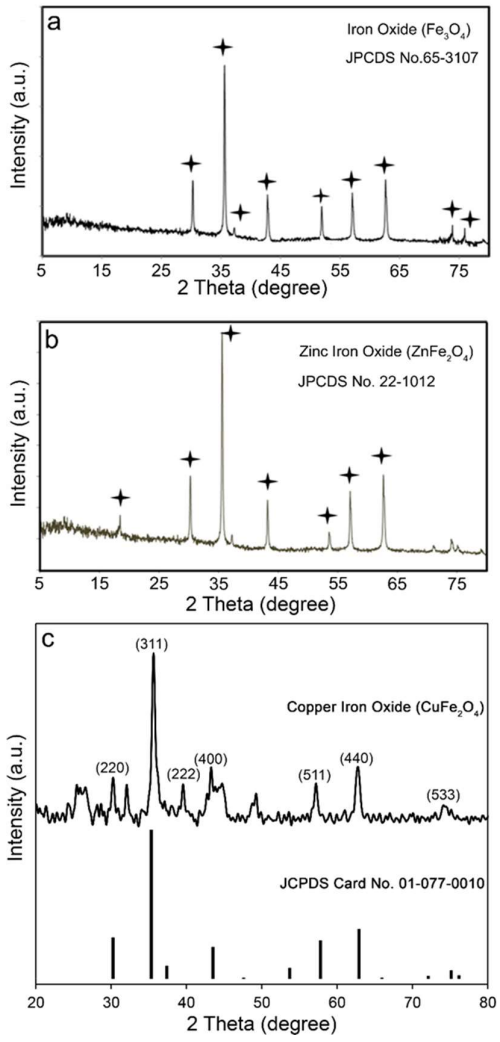

Fig. 4. XRD of (a) Fe_3O_4-BP-CH/FTO, (b) $ZnFe_2O_4$-BP-CH/FTO and (c) $CuFe_2O_4$-BP-CH/FTO

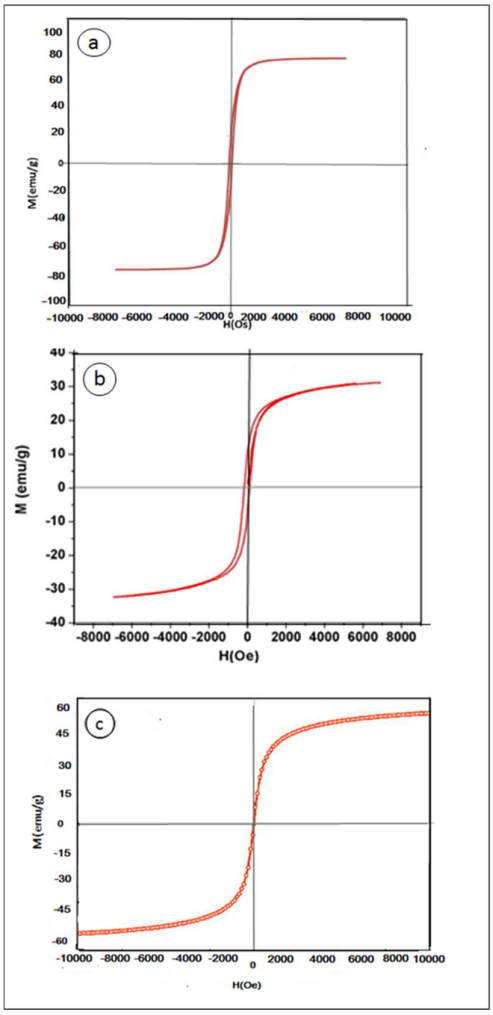

Fig. 5. VSM study of (a) $ZnFe_2O_4$-BP-CH, (b) $CuFe_2O_4$-BP-CH; (c) Fe_3O_4-BP-CH nanocomposites

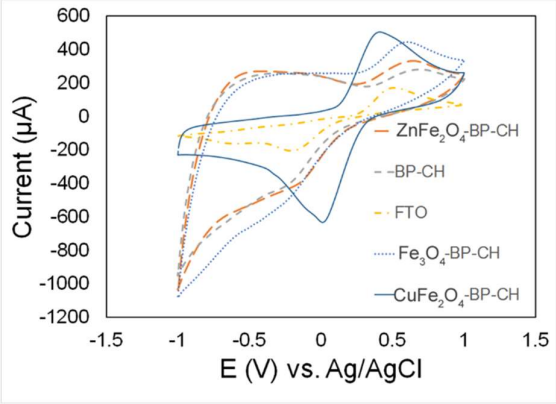

Fig. 6. CVs of the modified electrodes by BPs/different surfactants in 1 mM $K_3[Fe(CN)_6]$ and PBS 0.05 M (pH 7.4) at 100 mVs^{-1}

CV measurements show that the X-Fe_2O_4 incorporated nanocomposite, indicate fast electron transfer kinetics which based on relatively smallest ΔE and the largest peak current.

The magnitude of the peak current is increased for the $CuFe_2O_4$-BP-CH/FTO electrode than Fe_3O_4-BP-CH/FTO and $ZnFe_2O_4$-BP-CH/FTO, suggesting that the $CuFe_2O_4$ nanoparticle promote electron transfer in the CH and BP network at the electrode surface due to the good interaction between $CuFe_2O_4$ nanoparticles and CH-BP chain in the nanocomposite.

Fig. 7 exhibits the Nyquist plots of the BP-CH/CPE, $CuFe_2O_4$-BP-CH/FTO, $ZnFe_2O_4$-BP-CH/FTO and Fe_3O_4-BP-CH/FTO 1 mM $K_3[Fe(CN)_6]$ and PBS 0.05 M (pH 7.4). The EIS of the bare electrode shows 11000 Ω that is much more than the electrodes modified with different composites the electron transfer resistance in the modified electrodes decreases according to this pattern: bare FTO<BP-CH/FTO<Fe_3O_4-BP-CH/FTO<$NiFe_2O_4$-BP-CH/FTO<$CuFe_2O_4$-BP-CH/FTO (Table 1), which indicates that the $CuFe_2O_4$NPs show better electron transfer and conductivity in the composite. Therefore, the best composite, $CuFe_2O_4$-BP-CH/FTO, with resistance charge transfer 828 Ω was applied to the glucose biosensing.

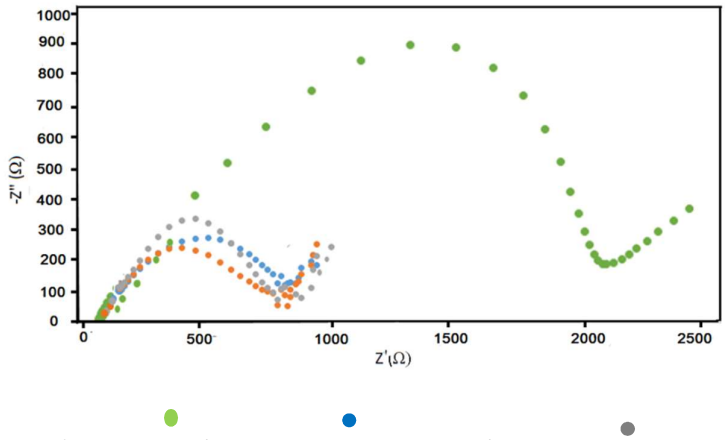

Fig. 7. EIS of composite BP-CH/FTO, $ZnFe_2O_4$-BP-CH/FTO, Fe_3O_4-BP-CH/FTO, $CuFe_2O_4$-BP-CH/FTO at 0.23 V with FTO as the working electrode and an Ag/AgCl/3.0 M as the reference electrode in electrochemical cell

Table 1. Comparison the EIS of the various types of X-Fe_2O_4-CH –BPs nanocomposites

Electrode	**resistance charge transfer (R_{ct}) (Ω)**
FTO	11000
BP-CH/FTO	1900
$CuFe_2O_4$-BP-CH/FTO	828
$ZnFe_2O_4$-BP-CH/FTO	880
Fe_3O_4-BP-CH/FTO	869

3.2. Biosensing application

Fig. 8 shows the amperometric response of the $CuFe_2O_4$-BP-CH/FTO electrode examined with several determined amount of glucose was added into PBS 0.05 M solutions. The calibration curve provides the regression equation, I (μA)=0.98$C_{glucose}$ (μM)+0.8, with correlation coefficient of R^2=0.99 (Fig. 8a). The electrode has a linear range of 0.25×10^{-3}–17×10^{-3} M, a sensitivity of 26330 μA$mM^{-1}cm^{-2}$, and a detection limit of 0.025 μM (2.5×10^{-8} M) (signal/noise=3).

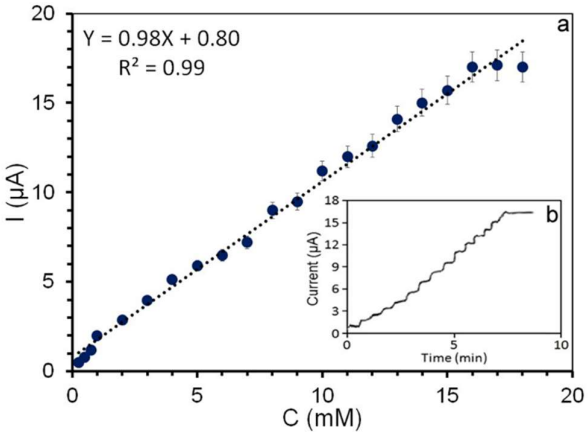

Fig. 8. Anodic peak current response (I_{pa}) *vs*. glucose concentration at high concentration. (0–18 mM) Insets plots of the glucose amperometric response of $CuFe_2O_4$-BP-CH/FTO examined in 0.1 M NaOH (pH 13) with sequential additions of glucose). E_{app}=+0.575 V

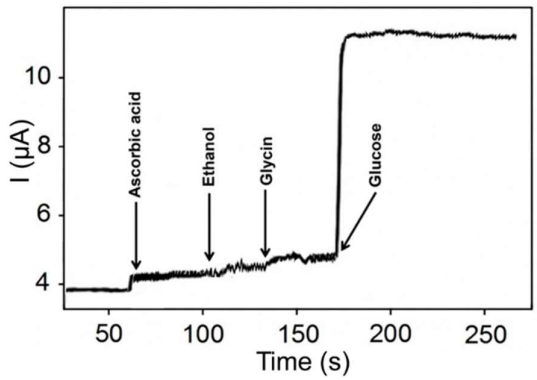

Fig. 9. Selectivity of $CuFe_2O_4$-BP-CH/FTO nanocomposite in PBS 0.05 M, (pH 7.4) with 10 mM interferents and 10 mM glucose

Selectivity is also important parameter in sensors performance. Some species, such as ascorbic acid (AA), ethanol, and glycine can play as a interfering species with glucose in human blood. The amperometric response of $CuFe_2O_4$-BP-CH/FTO was examined in PBS 0.05 M, (pH 7.4) with 10 mM interferents and 10 mM glucose. Insignificant responses were observed in Fig. 9 for interfering species which are less than the response of glucose that shows good

selectivity for glucose detection by using the $CuFe_2O_4$-BP-CH/FTO electrode. The longer term stability can be evaluated in the glucose solution intermittently which is an important factor in the performance of the biosensor. The result in Fig. 10 shows that the current response maintained more than 80% of its initial value after 28 days.

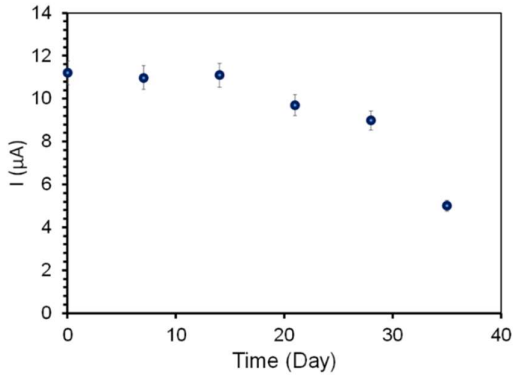

Fig. 10. Stability response of $CuFe_2O_4$-BP-CH/FTO nanocomposite after 35 days

4. CONCLUSION

According to the VSM, although $ZnFe_2O_4$ shows better response in magnetic environment individually and has high magnetic character, $CuFe_2O_4$ shows better performance in composite than the other ferrites and has a high quality interaction with BP and CH.

Table 2. Comparison of the $CuFe_2O_4$-BP-CH nanocomposite enzyme-free glucose sensor with other glucose sensors based on different material

Electrode	**Sensivity ($\mu A\ mM^{-1}cm^{-2}$)**	**Detection limit (μM)**	**Liner Range (M)**	**Ref.**
Chitosan-BP-$CuFe_2O_4$	26330	0.025	0.25×10^{-3}–17×10^{-3}	This work
Cu-MWCNT	922	2	0.5×10^{-3}–7.5×10^{-3}	[38]
$CuFe_2O_4$/rGO (30 wt%)	1824.22	1	0.6×10^{-3}–5.6×10^{-3}	[39]
Graphene/AuNPs/chitosan	-	180	2×10^{-3}_14×10^{-3}	[40]
Ppy-Chitosan-TiO_2	0.008	614	1×10^{-3}–14×10^{-3}	[41]
rGO/Ag	-	0.16	0.5×10^{-3}–12.5×10^{-3}	[42]
Ppy-Citosan-Fe_3O_4NP	12	234	1×10^{-3}–16×10^{-3}	[43]
Au NPs/Chitosan	99.5	370	0.4×10^{-3}–10.7×10^{-3}	[44]
Pt/AgTNPs/Chitosan	67.17	1	3×10^{-3}_3	[45]
Ti/Au/BP	20	10	Up to 9×10^{-3}	[22]
PB/MWNT	-	12.7	Up to 8×10^{-3}	[46]
BP-SWCNTs	21.5	0. 022 mM	Up to 10×10^{-3}	[47]

According to the table 2, $CuFe_2O_4$-CH-BP, a novel nonenzymatic glucose sensor, represents significant analytical characters, such as good sensitivity, strong stability, and

selectivity as well as short response times. The observed detection limit for this composite material is 0.025 μM with the linear range from of 0.25×10^{-3}–17×10^{-3} M. Table. 2 shows that, the sensitivity and detection limit of this electrode are better than those applied metals or metal oxide nanoparticles and CNT or graphene in their composites. So, it is a good result for using BP and its composites instead of graphene and CNT composite for biosensing application.

Briefly, we successfully synthesized the new X-Fe_2O_4-BP-CH nanocomposites on the electrode surface and also compared the interaction and electrochemical behavior of three nanoparticles with composite of BP and CH. In addition, we found a way to spread the application of $CuFe_2O_4$ as a suitable particle in biosensnig and also, fabricated a novel composite with BP that was more cost-effective nanocomposite than other enzyme-free glucose sensors. In future, we are thinking of adding some new materials to improve these properties as well.

Acknowledgements

The authors gratefully acknowledge the partial support from the Research Council of the Iran University of Science and Technology.

REFERENCES

[1] Y. Zare, J. Coll. Interf. Sci. 470 (2016) 245.
[2] Y. Zare, and K. Y. Rhee, Compos. Sci. Technol. 144 (2017) 18.
[3] R. Razavi, Y. Zare, and K. Y. Rhee, Coll. Surfaces A 538 (2018) 148.
[4] Y. Zare, and K. Y. Rhee, Compos. Sci. Technol. 155 (2018) 252.
[5] Y. Zare, and K. Y. Rhee, Composites Part A 100 (2017) 305.
[6] Y. Zare, K. Y. Rhee, and S. J. Park, Int. J. Adhes. Adhesiv. 79 (2017) 111.
[7] Y. Zare, Computat. Mater. Sci. 111 (2016) 334.
[8] S. M. Naghib, Micro. Nano Lett. 14 (2019) 462.
[9] E. Askari, S. M. Naghib, A. Seyfoori, A. Maleki, and M. Rahmanian, Ultrasonics Sonochem. (2019) 104615.
[10] R. Salahandish, A. Ghaffarinejad, S. M. Naghib, A. Niyazi, K. Majidzadeh-A, M. Janmaleki, and A. Sanati-Nezhad, Scientific Reports 9 (2019) 1226.
[11] S. Gooneh-Farahani, M. R. Naimi-Jamal, and S. M. Naghib, Expert Opinion on Drug Delivery 16 (2019) 79.
[12] A. Chen, and S. Chatterjee, Chem. Soc. Rev. 42 (2013) 5425.
[13] R. Salahandish, A. Ghaffarinejad, S. M. Naghib, K. Majidzadeh-A, and A. Sanati-Nezhad, IEEE Sens. J. 18 (2018) 2513.
[14] E. Askari, and S. M. Naghib, Int. J. Electrochem. Sci. 13 (2018) 886.

[15] S. M. Naghib, E. Parnian, H. Keshvari, E. Omidinia, and M. Eshghan-Malek, Int. .J Electrochem. Sci. 13 (2018) 1013.
[16] B. R. Adhikari, M. Govindhan, and A. Chen, Sensors 15 (2015) 22490.
[17] K. R. Mamaghani, S. M. Naghib, A. Zahedi, A. H. Z. Kalkhoran, and M. Rahmanian, Micro. Nano Lett. 13 (2018) 195.
[18] E. Omidinia, S. M. Naghib, A. Boughdachi, P. Khoshkenar, and D. K. Mills, Int. J. Electrochem. Sci. 10 (2015) 6833.
[19] S. M. Naghib, M. Rabiee, and E. Omidinia, Int. J. Electrochem. Sci. 9 (2014) 2301.
[20] R. Salahandish, A. Ghaffarinejad, S. M. Naghib, K. Majidzadeh-A, H. Zargartalebi, and A. Sanati-Nezhad, Biosens. Bioelectron. 117 (2018) 104.
[21] R. Salahandish, A. Ghaffarinejad, E. Omidinia, H. Zargartalebi, K. Majidzadeh-A, S. M. Naghib, and A. Sanati-Nezhad, Biosens. Bioelectron. 120 (2018) 129.
[22] A. Ahmadalinezhad, G. Wu, and A. Chen, Biosens. Bioelectron. 30 (2011) 287.
[23] J. Saberi, M. Ansari, B. E. Hoseinzadeh, S. S. Kordestani, and S. M. Naghib, Fiber. Polym.19 (2018) 2458.
[24] J. Singh, M. Srivastava, P. Kalita, and B. D. Malhotra, Process Biochem. 47 (2012) 2189.
[25] J. D. Qiu, H. Y. Xie, and R. P. Liang, Microchim. Acta 162 (2008) 57.
[26] Y. Li, X. Du, C. Wu, X. Liu, X. Wang, and P. Xu, Nanoscale Res. Lett. 8 (2013) 522.
[27] S. M. Naghib, M. Rahmanian, M. Keivan, S. Asiaei, and O. Vahidi, Int. J. Electrochem. Sci. 11 (2016) 10256.
[28] C. M. Welch, and R. G. Compton, Anal. Bioanal. Chem. 384 (2006) 601.
[29] N. Farsaei Vahid, M. Reza Marvi, M. Reza Naimi-Jamal, S. M. Naghib, and A. Ghaffarinejad, Micro & Nano Lett.13 (2018) 927.
[30] A. K. Gupta, and M. Gupta, Biomaterials 26 (2005) 3995.
[31] G. Zhao, J. J. Xu, and H. Y. Chen, Electrochem. Commun. 8 (2006) 148.
[32] A. Vijayalakshmi, Y. Tarunashree, B. Baruwati, S. Manorama, B. Narayana, R. Johnson, and N. Rao, Biosens. Bioelectron. 23 (2008) 1708.
[33] Y. Shen, Y. Wu, H. Xu, J. Fu, X. Li, Q. Zhao, and Y. Hou, Mater. Res. Bulletin 48 (2013) 4216.
[34] Z. Wang, H. Guo, Y. Yu, and N. He, J. Magnet. Magnet. Mater. 302 (2006) 397.
[35] K. Ali, A. Bahadur, A. Jabbar, S. Iqbal, I. Ahmad, and M. I. Bashir, J. Magnet. Mag. Mater. 434 (2017) 30.
[36] M. E. Assal, M. R. Shaik, M. Kuniyil, M. Khan, J. Kumar, A. Y. Alzahrani, A. Al-Warthan, S. A. Al-Tamrah, M. R. H. Siddiqui, and S. A. Hashmi, Mater. Express 8 (2018) 35.
[37] Y. Umasankar, D. B. Brooks, B. Brown, Z. Zhou, and R. P. Ramasamy, Adv. Energy Mater. 4 (2014).

[38] J. Zhao, L. Wei, C. Peng, Y. Su, Z. Yang, L. Zhang, H. Wei, and Y. Zhang, Biosens. Bioelectron. 47 (2013) 86.
[39] Z. Shahnavaz, P. M. Woi, and Y. Alias, Ceramics Int. 41 (2015) 12710.
[40] C. Shan, H. Yang, D. Han, Q. Zhang, A. Ivaska, and L. Niu, Biosens. Bioelectron. 25 (2010) 1070.
[41] A. Al-Mokaram, M. A. Amir, R. Yahya, M. M. Abdi, and H. N. M. E. Mahmud, Nanomaterials 7 (2017) 129.
[42] S. Palanisamy, C. Karuppiah, and S. M. Chen, Coll. Surfaces B: Biointerf. 114 (2014) 164.
[43] A. M. A. A. AL-Mokaram, R. Yahya, M. M. Abdi, and H. N. M. E. Mahmud, Mater. Lett. 183 (2016) 90.
[44] D. Feng, F. Wang, and Z. Chen, Sens. Actuators B 138 (2009) 539.
[45] W. Shi, and Z. Ma, Biosens. Bioelectron. 26 (2010) 1098.
[46] L. Zhu, J. Zhai, Y. Guo, C. Tian, and R. Yang, Electroanalysis 18 (2006) 1842.
[47] H. Papa, M. Gaillard, L. Gonzalez, and J. Chatterjee, Biosensors 4 (2014) 449.